Compton Scattering and Deep-Inelastic Electroproduction

B. H. Kellett
Department of Theoretical Physics, University of Manchester, Manchester, England
(Received 11 May 1972; revised manuscript received 20 July 1972)

A Regge-pole model for inelastic electroproduction and Compton scattering is presented. The coupling of the virtual photon to hadrons is assumed to be mediated by the known vector mesons. An additional k^2 dependence is postulated such that each Regge pole scales. The electroproduction structure functions are then scale-invariant, and excellent fits to the photon total cross section, Compton scattering, and inelastic-electroproduction data are obtained. Vector-meson dominance of the electromagnetic current is formulated covariantly in terms of the invariant amplitudes, and a central assumption of the model is that the invariant and helicity amplitudes continue smoothly to the gauge-invariant limit as the photon mass goes to zero. The additional assumption of s-channel helicity conservation for Compton scattering leads to the prediction that the ratio of longitudinal to transverse virtual-photon cross sections is $-m^2k^2/\nu^2$. It is observed that if Regge poles dominate the electroproduction cross section for c.m. energies above 2 GeV, in the scaling limit nonleading trajectories become important for small values of ω. Such nonleading effects are shown to be important for the fit to the ratio of electroproduction off neutrons and protons. For larger values of ω, the model suggests that the cross section is predominantly diffractive, so that νW_2 has essentially reached its asymptotic value by $\omega \simeq 20$. The form of the scale-invariance breaking for small $|k^2|$ is correctly predicted, and it is found that the deviations from scale invariance are not necessarily characterized by a small mass. Some points relating to the interpretation of the results of the model are discussed.

I. INTRODUCTION

It is well known that the original vector-meson-dominance (VMD) model proposed by Sakurai[1] for deep-inelastic electroproduction is in complete disagreement with the data.[2] The scaling behavior exhibited by this model arises from the dominance of the longitudinal-virtual-photon contribution for large values of $-k^2$, where k^2 is the mass of the virtual photon exchanged between the electron and the nucleon. The purely transverse-photon contribution does not scale, and becomes unimportant in the scaling region. The data on the other hand indicate that the transverse photons dominate the cross section, and present results are consistent with a small constant or zero ratio of longitudinal- to transverse-virtual-photon cross sections. Nevertheless, the success of VMD at small k^2 encourages the belief that the photon does interact with hadrons via an off-shell vector meson, and it is difficult to understand how the nature of the interaction can change dramatically by $k^2 \approx -1$ $(\mathrm{GeV}/c)^2$ where scaling behavior sets in. It is of some interest, therefore, to investigate the implications of scaling behavior for a model in which the photon couples to the hadrons via the vector-meson propagator. In this paper we present such a model in which the vector-meson-dominated electromagnetic current couples to a scale-invariant Regge-pole amplitude. The electroproduction structure functions are then scale-invariant, and the model gives a unified account of total cross sections for real photons, Compton scattering, and inelastic electroproduction for all spacelike values of k^2.

The main features of the deep-inelastic electroproduction cross section are now widely known. The extensive experimental and theoretical activity stimulated by the observation of scaling behavior in this reaction has been reviewed several times.[3] The structure functions for inelastic electroproduction are functions of ν and k^2, and it was suggested by Bjorken[4] that when ν and k^2 are much larger than any characteristic mass in the problem, the structure functions depend only on the ratio $\omega = -2\nu/k^2$. This scaling behavior finds its most natural explanation in terms of a basic pointlike interaction, and there has been a great deal of interest in parton[5] models which incorporate such a pointlike structure.[6,7]

Although parton models are attractive for their simple account of scaling behavior, they have the disadvantage that the prescription is rather different from the Regge-pole ideas normally associated with high-energy total cross sections. The work of Bloom and Gilman[8] and Rittenberg and Rubinstein[9] suggests that ideas familiar from purely hadronic reactions may have application to inelastic electroproduction. Ordinary Regge-pole models and Veneziano-like amplitudes have been considered by various authors,[10,11] and the model we shall present has some features in common with

the recent work of Moffat and Snell.[12] However, we wish to make the continuity with purely hadronic interactions more explicit by incorporating the concept of VMD. The simplest form of VMD is expressed by the ρ-photon analogy in which the hadronic interactions of the photon are mediated by an off-shell vector meson. Usually it is assumed that the corresponding vector-meson amplitude does not have any significant k^2 dependence, so that the dominant variation of the amplitude with k^2 comes from the vector-meson propagator. For inelastic electroproduction, however, such a model does not agree with the data, and it is essential that the vector-meson amplitude has sufficient k^2 dependence for the Regge-pole terms to scale by themselves. It might be argued that the introduction of such additional mass dependence destroys the applicability of VMD, but we feel that this is not necessarily the case. There are two points that can be made. First, the virtual photon is an external particle as far as the hadronic vertex is concerned, so the k^2 dependence associated with the electromagnetic current can be factored out of the amplitude. Moreover, we know that the electromagnetic current has a pole at the vector-meson mass, and there is no obvious reason why the effect of this pole should disappear for large spacelike k^2. Of course the simple propagator could be modified by the presence of additional contributions for timelike k^2, or by a new pointlike component that becomes important at large spacelike k^2. These possibilities have been investigated by several authors recently,[13] but in this work we shall use the concept of vector-meson dominance in the original sense suggested by the field-current identity, namely, that the electromagnetic current is dominated by the known vector-meson poles alone. The second important point to be made concerns the mass dependence of the resulting vector-meson scattering amplitude. The field-current identity itself tells us nothing about this additional k^2 dependence, and it is the simplifying assumption that the vector-meson amplitude does not vary appreciably as we go off shell that gives VMD its great predictive power. This assumption is reasonably successful over a limited range of k^2, but there is no reason in general for us to expect that a significant k^2 dependence may not be observed when we consider asymptotic values of k^2. The crucial point is that the mass dependence of the external photon is completely independent of the k^2 dependence of the vector-meson scattering amplitude, and it is perhaps unreasonable to throw away the effect of the known vector poles simply because they do not account for all the mass dependence.

In view of the failure of Sakurai's original model,[1] a new understanding of the relevance of VMD for inelastic electroproduction is clearly necessary. Some recent work[14,15] on the application of VMD at small $|k^2|$ has shown that it is advantageous to formulate VMD covariantly in terms of invariant amplitudes. The possibility of using more general structure functions to incorporate VMD in deep-inelastic electroproduction has been considered previously by Tung,[16] and in this paper we develop this idea and apply the general approach of Ref. 15 to the elastic scattering of real and virtual photons. We consider the effect of the current conservation constraints as $k^2 \to 0$, and by postulating the minimal k^2 dependence consistent with a smooth limit at $k^2 = 0$, we obtain relations between the real- and virtual-photon-invariant amplitudes. In a recent paper Akiba *et al.*[17] investigate the k^2 continuation in terms of helicity amplitudes. They find that a smooth $k^2 \to 0$ limit is consistent with the well-known singularity structure of the helicity amplitudes for both the massive and massless cases. Our approach is similar to theirs in some respects, but by emphasizing the central role of the invariant amplitudes, we are able to derive explicit relations between the different sets of invariant amplitudes appropriate to the massive and massless cases. The additional assumption of s-channel helicity conservation then gives the result $\sigma_L/\sigma_T = -m^2k^2/\nu^2$ for the longitudinal to transverse cross-section ratio, where ν is related to the energy loss of the electron. This result is independent of any particular assumption about VMD.

We then investigate the implications of scale invariance for a Regge-pole model for the invariant amplitudes in the presence of the vector propagator, and find that the additional k^2 dependence required is similar to that required by traditional scale-invariant Regge models.[10,12] In these models each Regge pole scales separately, so we achieve a more general scale invariance than is present in other VMD models,[13] where only the asymptotic Pomeranchukon contribution scales. The price we have to pay for this is contained in the k^2 dependence of the off-shell vector-meson scattering amplitude. However, it is possible to look on inelastic electroproduction as the way in which this mass dependence is to be measured in the spacelike region. It is not necessary for the k^2 dependence to be the same for $k^2 > 0$, but the consequences of a simple continuation could be tested by investigating the mass dependence of photoproduced electron or muon pairs for instance.

Since our model gives a smooth $k^2 \to 0$ limit, in addition to obtaining excellent fits to the data both in the scaling limit and at $k^2 = 0$, we are able to account for the scale-invariance breaking observed at small k^2. We find that the interpretation of the

data provided by this model differs in some respects from the results of other models. In particular the model gives Regge behavior for the electroproduction structure functions for all ω, as long as the c.m. energy is above 2 GeV. Furthermore, the diffractive contribution dominates the cross section for $\omega \gtrsim 5$ in the scaling limit. In principle our model can be extended to include vector-meson photoproduction and electroproduction, and vector-meson scattering on nucleons, but this possibility is not followed up here.

The paper is divided into six sections. In Sec. II we discuss the notation we shall employ and define the electroproduction cross section and structure functions. The general invariant amplitudes are introduced in Sec. III, and the continuation to $k^2=0$ is discussed. In Sec. IV the various points bearing on the dynamical k^2 dependence necessary for scaling behavior are considered, and we construct a dynamical model for the invariant amplitudes. The fit to the data is presented in Sec. V and various points in the interpretation of the results are raised. The final section (Sec. VI) is given over to a summary and brief discussion of the model.

II. NOTATION AND KINEMATICS

In general, virtual Compton scattering from nucleons

$$\gamma_\lambda(k)+N(p)\to\gamma_\mu(k')+N(p') \tag{2.1}$$

is described by 18 independent helicity amplitudes. For elastic scattering, $k^2=k'^2$ and time-reversal invariance reduces the number of independent amplitudes to 12. In the particular case of real Compton scattering, the additional constraint of gauge invariance eliminates the longitudinal polarization states of the photon and leaves only six independent amplitudes. The differential cross section is given by

$$\frac{d\sigma}{dt}=\frac{1}{64\pi\sigma|\vec{k}_c|^2 s}\sum_{\lambda_i}|f_{\lambda_i}|^2, \tag{2.2}$$

where σ is the number of initial spin states, and $|\vec{k}_c|$ is the center-of-mass momentum.

In general the total absorption cross section consists of two parts, σ_L and σ_T, coming from longitudinal and transverse photons, respectively. The optical theorem relates the total cross section to the imaginary part of the spin-averaged forward amplitude:

$$\sigma_L=-\frac{1}{2|\vec{k}_c|W}\,\mathrm{Im}f_{0\frac12,0\frac12}(\theta=0^\circ), \tag{2.3}$$

$$\sigma_T=-\frac{1}{4|\vec{k}_c|W}\,\mathrm{Im}(f_{1\frac12,1\frac12}+f_{1-\frac12,1-\frac12})(\theta=0^\circ), \tag{2.4}$$

where W is the c.m. energy, $W^2=s$. Once again, for real photons at $k^2=0$ only the transverse contribution σ_T^γ survives. The superscript γ will be used throughout to distinguish the real photon amplitudes and cross section from those for virtual photons.

For inelastic electroproduction $e+p\to e+$anything, we use the one-photon-exchange approximation and define the variables

$$k^2=(p_e-p_e')^2 = -4EE'\sin^2(\tfrac12\theta), \tag{2.5}$$

$$\nu=p\cdot k = m(E-E'), \tag{2.6}$$

where p_e, p_e' are the initial and final electron momenta, E, E' their energies, and θ is the electron scattering angle in the laboratory. The variable[18] ν is related to the c.m. energy of the hadronic system by

$$2\nu=s-m^2-k^2. \tag{2.7}$$

Inelastic electroproduction can be described in terms of the spin-averaged forward amplitude

$$W_{\lambda\mu}=\frac{1}{4\pi}\int d^4x\, e^{ik\cdot x}\langle p|[J_\lambda(x),J_\mu(0)]|p\rangle, \tag{2.8}$$

where J_μ is the electromagnetic current. Conventionally this amplitude is decomposed into two structure functions,

$$W_{\lambda\mu}=-\left(g_{\lambda\mu}-\frac{k_\lambda k_\mu}{k^2}\right)W_1(\nu,k^2) +\frac{1}{m^2}\left(p_\lambda-k_\lambda\frac{p\cdot k}{k^2}\right)\left(p_\mu-k_\mu\frac{p\cdot k}{k^2}\right)W_2(\nu,k^2). \tag{2.9}$$

In this form the current conservation constraints

$$k^\lambda W_{\lambda\mu}=k^\mu W_{\lambda\mu}=0$$

are explicitly satisfied, but the structure functions have kinematic zeros. In order that $W_{\lambda\mu}$ remain finite at $k^2=0$, we must have

$$W_2\sim O(k^2),\qquad \left(W_1+\frac{\nu^2}{m^2k^2}W_2\right)\sim O(k^2) \tag{2.10}$$

as $k^2\to 0$.

The electron scattering cross section is then given by

$$\frac{d^2\sigma}{d\nu d|k^2|}=\frac{4\pi\alpha^2}{m^2k^4}\frac{E'}{E} \times[2\sin^2(\tfrac12\theta)W_1(\nu,k^2)+\cos^2(\tfrac12\theta)W_2(\nu,k^2)]. \tag{2.11}$$

This differential cross section can also be written in terms of the total cross sections for virtual photons σ_L and σ_T:

$$\frac{d^2\sigma}{d\nu d|k^2|} = \frac{\alpha}{2\pi}\frac{\nu+\frac{1}{2}k^2}{m^2E^2k^2}\frac{1}{1-\epsilon}(\sigma_T+\epsilon\sigma_L), \tag{2.12}$$

where ϵ is the polarization of the virtual photon,

$$\epsilon = \left[1+2\left(1-\frac{\nu^2}{m^2k^2}\right)\tan^2(\tfrac{1}{2}\theta)\right]^{-1}. \tag{2.13}$$

By convention, the flux factor for σ_L and σ_T in Eq. (2.12) is taken to be that for real photons, $2|\vec{k}_c|W = 2\nu + k^2$. Comparing Eqs. (2.11) and (2.12) we immediately obtain the relations

$$W_1 = \frac{\nu+\frac{1}{2}k^2}{4\pi^2\alpha}\sigma_T, \qquad W_2 = \frac{\nu+\frac{1}{2}k^2}{4\pi^2\alpha}\frac{k^2m^2}{k^2m^2-\nu^2}(\sigma_L+\sigma_T). \tag{2.14}$$

Scaling in the sense of Bjorken[4] means that as k^2 tends to infinity with the ratio $\omega = -2\nu/k^2$ fixed, the structure functions W_1 and $\nu W_2/m^2$ become functions of ω alone:

$$\lim_{k^2\to-\infty} 2W_1(\nu,k^2) \to F_1(\omega), \qquad \lim_{k^2\to-\infty}\frac{\nu}{m^2}W_2(\nu,k^2)\to F_2(\omega). \tag{2.15}$$

This scaling behavior has been observed in the data,[2] and determines many of the features of the model we shall present.

III. INVARIANT AMPLITUDES AND THE CONTINUATION TO $k^2 = 0$

It is well known that the helicity decomposition of a massive vector particle is Lorentz-frame-dependent and that this gives rise to a basic ambiguity in the application of the hypothesis of vector-meson dominance. The longitudinal and transverse virtual-photon cross sections in Sec. II refer to the helicity frame, but in order to introduce VMD in a covariant manner we shall follow the approach of Refs. 14 and 15 and define invariant amplitudes for real and virtual Compton scattering. Since we are interested only in total cross sections for virtual photons, we limit our discussion to elastic scattering for which $k^2 = k'^2$. Time-reversal invariance then simplifies the problem considerably.

We consider first the case $k^2 \neq 0$. The same invariant amplitudes are applicable for both spacelike and timelike k^2, and we find that with the momenta at our disposal we can construct 22 covariants. Of these, however, eight involve terms like $k_\mu\epsilon^\mu(k)$, where $\epsilon^\mu(k)$ is the polarization vector for the particle of momentum k. By current conservation, such terms do not contribute to the physical cross section. The two covariants $(P_\lambda k_\mu + k'_\lambda P_\mu)\not{Q}$ and $k'_\lambda k_\mu \not{Q}$, where $P \equiv \frac{1}{2}(p'+p)$ and $Q \equiv \frac{1}{2}(k'+k)$, are eliminated by the equivalence theorems[19] given in the Appendix. This leaves the required 12 invariant amplitudes that are free from kinematic singularities and zeros (KSZF). The set we choose can be defined in terms of the T matrix,

$$T = \bar{u}(p')M_{\lambda\mu}\epsilon^\lambda(k)\epsilon^\mu(k')u(p), \tag{3.1}$$

where

$$\begin{aligned} M_{\lambda\mu} = {} & P_\lambda P_\mu C_1 + P_\lambda P_\mu \not{Q} C_2 + k'_\lambda k_\mu C_3 + (P_\lambda k_\mu + k'_\lambda P_\mu)C_4 + g_{\lambda\mu}C_5 + g_{\lambda\mu}\not{Q}C_6 + (\gamma_\lambda P_\mu + P_\lambda\gamma_\mu)C_7 + (\gamma_\lambda k_\mu + k'_\lambda\gamma_\mu)C_8 \\ & + (P_\lambda\not{Q}\gamma_\mu + \gamma_\lambda\not{Q}P_\mu)C_9 + (\gamma_\lambda\not{Q}k_\mu + k'_\lambda\not{Q}\gamma_\mu)C_{10} + (\gamma_\lambda\gamma_\mu - \gamma_\mu\gamma_\lambda)C_{11} + (\gamma_\lambda\not{Q}\gamma_\mu - \gamma_\mu\not{Q}\gamma_\lambda)C_{12}. \end{aligned} \tag{3.2}$$

These invariant amplitudes are essentially the set given by Scadron and Jones.[19]

It is rather more difficult to find a KSZF set of invariant amplitudes for Compton scattering. Because of the gauge-invariance constraints, there are only six independent amplitudes, but introducing gauge invariance in any simple way also introduces kinematic singularities and zeros. We saw in Sec. II that the standard gauge-invariant definition of W_1 and W_2 leaves these quantities with constraints and zeros at $k^2 = 0$. The problem has, however, been solved[20] and we shall use the amplitudes defined by

$$\begin{aligned} M_{\lambda\mu} = {} & (k\cdot k' g_{\lambda\mu} - k'_\lambda k_\mu)A_1 + [k\cdot k' P_\lambda P_\mu - \nu(P_\lambda k_\mu + k'_\lambda P_\mu) + \nu^2 g_{\lambda\mu}]A_2 \\ & + [k\cdot k'(P_\lambda\gamma_\mu + \gamma_\lambda P_\mu) - \nu(k'_\lambda\gamma_\mu + \gamma_\lambda k_\mu) + (2\nu g_{\lambda\mu} - P_\lambda k_\mu - k'_\lambda P_\mu)\not{Q}]A_3 \\ & + [4P_\lambda P_\mu\not{Q} - 2\nu(P_\lambda\gamma_\mu + \gamma_\lambda P_\mu) - \nu(\gamma_\lambda\not{Q}\gamma_\mu - \gamma_\mu\not{Q}\gamma_\lambda)]A_4 \\ & + [k\cdot k'(\gamma_\lambda\gamma_\mu - \gamma_\mu\gamma_\lambda) - k'_\lambda(\not{k}\gamma_\mu - \gamma_\mu\not{k}) - k_\mu(\gamma_\lambda\not{k}' - \not{k}'\gamma_\lambda) + 4g_{\lambda\mu}(m\not{Q} - \nu)]A_5 \\ & + [k\cdot k'(\gamma_\lambda\not{Q}\gamma_\mu - \gamma_\mu\not{Q}\gamma_\lambda) - 2\not{Q}(P_\lambda k_\mu + k'_\lambda P_\mu) + 2\nu(\gamma_\lambda k_\mu + k'_\lambda\gamma_\mu)]A_6. \end{aligned} \tag{3.3}$$

In general, for $k^2 = k'^2$

$$2\nu = 2k \cdot P$$
$$= s - m^2 - k^2 + \tfrac{1}{2}t, \tag{3.4}$$
$$k \cdot k' = k^2 - \tfrac{1}{2}t\ , \tag{3.5}$$

and in Eqs. (2.7) and (3.3) we have the particular cases $t=0$ and $k^2=0$, respectively. Once again for Compton scattering there are two further covariants that are eliminated by the equivalence theorems. Since these covariants are rather cumbersome, they are defined in the Appendix together with the appropriate equivalence theorems.

The invariant amplitudes defined by Eqs. (3.2) and (3.3) form the basis for our argument concerning the continuation in k^2, and it is of some importance that the reasons for this particular choice be understood. The most important consideration is that these amplitudes are KSZF. They have simple crossing properties, and are not constrained at thresholds or the boundaries of the physical region. Consequently the analytic structure of the invariant amplitudes is entirely determined by the dynamics, and we can write simple dispersion relations for them. These properties are of particular importance in our work where we require the k^2 continuation to be smooth, with no discontinuities at $k^2=0$. One can prove that the amplitudes are free from singularities and constraints by considering their relation to helicity amplitudes. The singularities and constraints for helicity amplitudes are known, and it is possible to check the KSZF structure of the invariant amplitudes explicitly. Alternatively, one can follow Hearn[21] and start from the fact that the complete set of possible covariants and invariant amplitudes cannot have singularities. Consequently any nonredundant set will share this property provided no singularities are introduced by the reduction. This reduction involves equivalence theorems such as those given in the Appendix, and other simple relations arising from momentum conservation and identities between γ matrices. Notice that the proof of KSZF structure for the C_i is independent of k^2 except for the point $k^2=0$. Thus, with the possible exception of this point, these amplitudes do not have singularities or zeros in k^2. We shall consider the structure of the C_i at $k^2=0$ in the latter part of this section.

The other important consideration in our choice of KSZF amplitudes is that they should be unique. At first sight the amplitudes defined by Eqs. (3.2) and (3.3) do not appear to be unique simply because any linear combination with constant numerical coefficients will have the same analytic properties. On the other hand, a linear transformation with coefficients depending on the kinematic variables will introduce singularities whenever the determinant of the transformation vanishes. But if the determinant is a constant, the new set of amplitudes provides a possible basis. If the linear transformation connecting two possible sets of amplitudes is nonsingular, the inverse transformation exists everywhere, and it is relatively simple to show that in this case the different sets of amplitudes lead to equivalent physical results. This follows from the fact that when reciprocal relations between the different sets of amplitudes are uniquely defined everywhere, it is always possible to translate from one set of amplitudes to the other. It is only in the presence of kinematical singularities, where the transformation is singular, that the physical results need not be equivalent, and we consider this to be sufficient reason for considering only KSZF amplitudes for which unique results are possible.

It should be pointed out that the gauge-invariant Compton amplitudes of Eq. (3.3) are KSZF for $k^2=0$ only. For k^2 different from zero we have the weaker constraints of current conservation, and the real Compton amplitudes develop kinematic singularities. In general, the 12 non-gauge-invariant amplitudes are completely independent except at $k^2=0$ where they must assume gauge-invariant form. The central assumption of our use of these amplitudes is that this transition to $k^2=0$ is smooth. The simplest way to implement this assumption is to expand the amplitudes C_i as a power series in k^2. The zeroth-order terms of this expansion are given by the gauge-invariant structure at $k^2=0$, and these terms are readily obtained by equating the M functions (3.2) and (3.3) at $k^2=0$.

This leads to

$$\begin{aligned}
&C_1 = k\cdot k' A_2, && C_2 = 4A_4,\\
&C_3 = -A_1 + 2A_5, && C_4 = -\nu A_2 - m(A_3 + 2A_6) + 2A_5,\\
&C_5 = k\cdot k' A_1 + \nu^2 A_2 - 4\nu A_5, && C_6 = 2\nu A_3 + 4mA_5,\\
&C_7 = k\cdot k' A_3 - 2\nu A_4, && C_8 = -2\nu A_3 - 2mA_5,\\
&C_9 = 2m(A_3 + 2A_6), && C_{10} = -2A_5,\\
&C_{11} = -m\nu(A_3 + 2A_6) + k\cdot k' A_5, && C_{12} = -P^2(A_3 + 2A_6) - \nu A_4 + k\cdot k' A_6,
\end{aligned} \tag{3.6}$$

where $P^2 = m^2 - \frac{1}{4}t$. The invariants $k \cdot k'$ and ν in Eq. (3.6) are at this stage to be evaluated at $k^2 = 0$.

In order to say anything about the k^2 dependence of the C_i we must look at other constraints on the amplitudes. In the case of pion photo- and electroproduction it was found that the corresponding zeroth-order expansion was all that was necessary.[15] Current conservation imposes two constraints on the eight non-gauge-invariant amplitudes introduced by Ball.[22] These constraints are linear in k^2, and Cho and Sakurai[14] pointed out that the assumption that the Ball amplitudes are independent of k^2 introduces only two further constraints. These four constraints leave just four independent amplitudes, which is the number required in the gauge-invariant photoproduction limit. Equating the Ball amplitudes to the gauge-invariant set at $k^2 = 0$ then imposes a structure for k^2 different from zero such that the current conservation constraints are automatically satisfied for all k^2, and the pion electroproduction helicity amplitudes continue smoothly to the corresponding photoproduction amplitudes as $k^2 \to 0$.

We now look at the implications of similar arguments for real and virtual Compton scattering. We can see immediately that the C_i of Eq. (3.2) cannot be independent of k^2. There are 20 independent amplitudes if we use the equivalence theorems, but do not impose the Lorentz condition. These amplitudes must satisfy eight current conservation constraints as expected. These constraints are again linear in k^2, so if we assume that the C_i are independent of k^2, there are 16 constraints on the 20 amplitudes. Therefore, in order for there to be six independent amplitudes at $k^2 = 0$, we must allow the C_i to contain terms at least proportional to k^2. Some information on these terms can be obtained by considering the helicity amplitudes. In addition to the requirement that the invariant amplitudes continue smoothly to $k^2 = 0$, we demand that the helicity amplitudes also are well behaved in this limit. In other words, the longitudinal helicity amplitudes $f_{0\lambda,0\lambda'} \sim O(k^2)$ and $f_{0\lambda,1\lambda'} \sim O((|k^2|)^{1/2})$, and the transverse amplitudes must go over into the corresponding real Compton amplitudes.

We give the expansion of the s-channel helicity amplitudes in terms of the invariant amplitudes for both the real and virtual elastic processes in the Appendix. By direct substitution of Eqs. (3.6) into Eqs. (A9), we find that the transverse and $f_{0\lambda,1\lambda'}$ amplitudes continue as required when $k^2 \to 0$, but the longitudinal amplitudes $f_{0\lambda,0\lambda'}$ do not vanish as k^2. It can be readily verified, however, that the correct behavior is obtained if the kinematical factors $k \cdot k'$ and ν in Eqs. (3.6) are allowed the natural k^2 dependence of Eqs. (3.4) and (3.5). In fact, inspection of the constraints shows that this is the only allowed k^2 dependence that does not introduce spurious singularities. There are no similar constraints on terms of $O(k^4)$ and higher in the expansion. Consequently, such terms are completely arbitrary, and can be restricted only by physical considerations. The approach of Ref. 15 was to assume minimal k^2 dependence, and this approach will be followed here. From the above discussion it follows that the minimal k^2 dependence of the C_i is given by Eqs. (3.6), together with (3.4) and (3.5).

If we now restrict ourselves to the forward direction $t = 0$, we see from Eqs. (A9) that the surviving helicity amplitudes for spacelike virtual photons are

$$\begin{aligned} f_{0\frac{1}{2},0\frac{1}{2}} &= -\frac{2}{k^2}\left[|\vec{k}_C|^2 s\,(mC_1 + 2\dot{C}_7)\right. \\ &\qquad \left. + \nu(|\vec{k}_C|^2 s C_2 - k^2 C_6) - mk^2 C_5\right], \\ f_{0-\frac{1}{2},1\frac{1}{2}} &= -\frac{2\sqrt{2}}{(-k^2)^{1/2}}(|\vec{k}_C|^2 s C_9 + 2\nu C_{11} + 2mk^2 C_{12}), \\ f_{1\frac{1}{2},1\frac{1}{2}} &= -2[m(C_5 - 2C_{11}) + \nu(C_6 + 2C_{12})], \\ f_{1-\frac{1}{2},1-\frac{1}{2}} &= -2[m(C_5 + 2C_{11}) + \nu(C_6 - 2C_{12})]. \end{aligned} \tag{3.7}$$

Similarly, for real photons at $t = 0$, the helicity amplitudes are given from Eqs. (A10):

$$\begin{aligned} f^{\gamma}_{1\frac{1}{2},1\frac{1}{2}} &= -(s - m^2)^2(\tfrac{1}{2}mA_2 + A_3 - A_4), \\ f^{\gamma}_{1-\frac{1}{2},1-\frac{1}{2}} &= -(s - m^2)^2(\tfrac{1}{2}mA_2 + A_3 + A_4). \end{aligned} \tag{3.8}$$

Notice that from a consideration of the forward direction alone it would appear that the smoothness constraints are much more easily satisfied. We can obtain smooth relations between Eqs. (3.7) and (3.8) for which the amplitudes C_i do not depend on k^2. Because of this it is important to remember that the k^2 continuation must hold for all t, and it is unwise to draw conclusions from the k^2 dependence of the forward helicity amplitudes by themselves.

The total absorption cross section for real photons is proportional to the imaginary part of

$$f^{\gamma}_{1\frac{1}{2},1\frac{1}{2}} + f^{\gamma}_{1-\frac{1}{2},1-\frac{1}{2}} = -(s - m^2)^2(mA_2 + 2A_3). \tag{3.9}$$

From Eqs. (3.6) and (3.7), we can rewrite the forward spin-averaged spacelike-photon amplitudes in the form

$$f_{0\frac{1}{2},0\frac{1}{2}} = 2mk^2[A_1 + m(mA_2 + 2A_3)], \tag{3.10}$$

$$f_{1\frac{1}{2},1\frac{1}{2}} + f_{1-\frac{1}{2},1-\frac{1}{2}} = -4[mk^2 A_1 + \nu^2(mA_2 + 2A_3)], \tag{3.11}$$

which clearly satisfies the conditions that $f_{0\frac{1}{2},0\frac{1}{2}}$ vanishes as k^2, and $f_{1\frac{1}{2},1\frac{1}{2}} + f_{1-\frac{1}{2},1-\frac{1}{2}}$ reduces to Eq. (3.9) at $k^2 = 0$.

We now consider the asymptotic behavior of

these amplitudes. Regge theory predicts that helicity amplitudes $\sim\nu^{\alpha}$ as $\nu\to\infty$. This implies $A_{1,6}\sim\nu^{\alpha}$, $A_5\sim\nu^{\alpha-1}$, and $A_{2,3,4}\sim\nu^{\alpha-2}$. We might expect, therefore, that $f_{0\frac{1}{2},0\frac{1}{2}}$ is dominated by A_1, but this leads to problems. Since A_1 enters Eqs. (3.10) and (3.11) with opposite signs, the positivity of the total cross section is not guaranteed when A_1 dominates. This problem for the k^2 continuation has previously been noticed by Tung,[16] and he suggested a solution that involved the introduction of kinematical singularities far from the physical region. However, we know that by construction the C_i cannot have such singularities, and the simplest solution would seem to be to assume that terms of $O(k^4)$ in the continuation enter in such a way that positivity for the total cross section is assured. It is easy to check that in any given case it is possible to introduce a suitable k^2 dependence. However, this destroys the concept of minimal k^2 dependence for the invariant amplitudes and introduces complete arbitrariness. If we wish to make progress, it is necessary to find some physical limitation on this freedom. Fortunately, the simple physical consideration of s-channel helicity conservation suggests a more clearly defined prescription for ensuring the positivity of the total cross section. At sufficiently high energies, the real Compton amplitudes simplify to

$$\begin{aligned}
&f^{\gamma}_{1\frac{1}{2},1\frac{1}{2}} = -s^2(\tfrac{1}{2}mA_2 + A_3 - A_4),\\
&f^{\gamma}_{1-\frac{1}{2},1-\frac{1}{2}} = -s^2(\tfrac{1}{2}mA_2 + A_3 + A_4),\\
&f^{\gamma}_{1\frac{1}{2},1-\frac{1}{2}} = \tfrac{1}{4}s^2(-t)^{1/2}A_2,\\
&f^{\gamma}_{1\frac{1}{2},-1\frac{1}{2}} = mtA_1,\\
&f^{\gamma}_{1\frac{1}{2},-1-\frac{1}{2}} = -\tfrac{1}{2}(-t)^{1/2}(tA_1 + 8sA_5 + 2mtA_6),\\
&f^{\gamma}_{1-\frac{1}{2},-1\frac{1}{2}} = \tfrac{1}{2}t(-t)^{1/2}(A_1 - 2mA_6).
\end{aligned} \tag{3.12}$$

Thus if we impose s-channel helicity conservation (SCHC), the only invariant amplitudes to survive at high energies are A_3 and A_4. The evidence for SCHC comes primarily from vector-meson photoproduction,[23] but the recent experiment of Buschhorn *et al.*[24] on Compton scattering with polarized photons is certainly consistent with the zero asymmetry predicted by SCHC. Moreover, for Compton scattering, zero asymmetry is an unambiguous indication of SCHC, without the alternative explanations of the density-matrix measurements possible in vector photoproduction.[25]

In particular, SCHC implies that the amplitude A_1 is small, and has an energy dependence one or two powers of ν below its possible ν^{α} form. Consequently, the k^2 dependence necessary to maintain positivity is not important, and it is a reasonable approximation to take $A_1=0$. Furthermore, since A_4 is dominated by unnatural-parity exchange, it is a reasonable approximation to assume that it vanishes as well. Provided $A_1=0$, assuming that only A_3 is nonzero does not lead to any loss of generality for the spin-averaged forward amplitude, but it is a stronger assumption away from the forward direction where the pion contributes to A_6, for instance. In this work, however, we shall use the simplified model in which A_3 is the dominant amplitude for all t. The virtual-photon total cross sections can then be very simply written as

$$\sigma_L = -\frac{2m^2k^2}{\nu+\frac{1}{2}k^2}\,\mathrm{Im}A_3, \tag{3.13}$$

$$\sigma_T = \frac{2\nu^2}{\nu+\frac{1}{2}k^2}\,\mathrm{Im}A_3, \tag{3.14}$$

where we have followed the convention of using the flux factors appropriate for real photons. The real photoabsorption cross section becomes, from Eq. (3.14),

$$\sigma^{\gamma}_T = (s-m^2)\,\mathrm{Im}A_3. \tag{3.15}$$

An immediate consequence of Eqs. (3.13) and (3.14) is that the ratio of longitudinal to transverse cross sections for virtual photons is

$$R \equiv \frac{\sigma_L}{\sigma_T} = -\frac{m^2k^2}{\nu^2}. \tag{3.16}$$

This result is independent of any considerations of vector dominance, and is a direct consequence of our assumptions of s-channel helicity conservation for Compton scattering and minimal k^2 dependence of the C_i. The form (3.16) for R is equivalent to the statement that the matrix elements for transverse and longitudinal photons are equal, and it is perfectly consistent with the present data on deep-inelastic electroproduction. It is a natural consequence of the present approach to the k^2 continuation, whereas such a form for R is difficult to understand in terms of parton models, and Moffat and Snell[12] for instance, have to assume this result before they can relate Compton scattering to inelastic electroproduction.

A further consequence of the relation (3.6) between the real and virtual Compton amplitudes is the prediction that the Pomeranchukon decouples from longitudinal vector mesons. Since Eqs. (3.6) hold for positive as well as negative values of k^2, the result Eq. (3.16) applies also to vector-meson cross sections, and the longitudinal to transverse ratio for ρN scattering, for instance, will go down like $m^2m_\rho{}^2/\nu^2$. This contradicts spin independence at high energies, and it would be of some interest to check experimentally whether the observed dominance of the transverse cross section for spacelike k^2 holds at the vector-meson mass also.

IV. THE DYNAMICAL MODEL

So far we have been primarily concerned with the kinematic structure of the invariant amplitudes; with the introduction of dynamical concepts such as SCHC only insofar as was necessary to limit kinematic freedom. However, the invariant amplitudes can have additional k^2 dependence arising from the dynamics, and we shall investigate this in terms of a particular Regge-pole model.

From Eqs. (2.14), (3.13), and (3.14) we obtain the relations between the scale-invariant electroproduction structure functions and A_3,

$$W_1 = \frac{\nu^2}{2\pi^2\alpha}\,\mathrm{Im}A_3\,, \tag{4.1}$$

$$\frac{\nu}{m^2}W_2 = -\frac{k^2\nu}{2\pi^2\alpha}\,\mathrm{Im}A_3\,. \tag{4.2}$$

The amplitude A_3 receives contributions from the natural-parity t-channel exchanges P, f, and A_2. The pion trajectory can also be exchanged, and this contributes to the amplitude A_6. The coupling $\pi^0 \to \gamma\gamma$ is small compared with the Pomeranchukon coupling implied by the total photoabsorption cross section, however, and we shall not consider this unimportant contribution to the Compton differential cross section further. There are several independent points to be considered in connection with the form of the Regge amplitude, and we shall deal with them in turn.

A. Vector-Meson Dominance

In the vector-dominance model, the hadronic interactions of the photon are identified with the interactions of an off-shell vector meson. For general Compton scattering, the field-current identity gives the relation

$$A(k^2) = \left(\frac{m_V^2}{m_V^2 - k^2}\right)^2 A^V(k^2)\,, \tag{4.3}$$

where m_V is the vector mass, and A^V is the amplitude for elastic scattering of vector mesons from nucleons. As we discussed in the Introduction, we depart from the strict vector-dominance approach by allowing the vector-meson amplitude to depend on k^2. The importance of Eq. (4.3) is that it accounts for the factorizable k^2 dependence of the vector-meson propagator, present when the photon coupling to hadrons is dominated by the known vector mesons, and reproduces the pole at $k^2 = m_V^2$. The k^2 dependence of A^V allows us to write Eq. (4.3) either for the real Compton invariant amplitudes A_i, or for the vector-meson amplitudes C_i. The remaining k^2 dependence of these amplitudes is to be determined by the requirement of scale invariance in the deep-inelastic region.

Since we are interested in the large spacelike k^2 region, we are a long way from the vector-meson poles, and it might be expected in general that this propagator could be modified by timelike states of mass higher than the ρ. Even if there are no vector-meson poles above the ρ, ω, and ϕ states, nonresonant continuum contributions may be important. The simplest possibility is to allow m_V in Eq. (4.3) to vary, but we found in fact that these effects are not very important, and perfectly adequate fits to the data were obtained with $m_V = m_\rho$. We have used the approximation $m_\rho = m_\omega$, and have neglected the small ϕ contribution. Since we do not go to the vector-meson pole, the direct ρ-γ coupling does not enter, and the relative normalization of the Compton and electroproduction results are fixed in the scaling limit by m_V and the Regge scale factor.

B. Implications of Scale Invariance

It was pointed out in the Introduction that Regge models do not predict scale invariance. We must use the fact of scale invariance as exhibited by the data to determine the form of Regge exchange for variable k^2. From Eqs. (4.2) and (4.3) we find that as $k^2 \to -\infty$

$$\frac{\nu}{m^2}W_2 \to \frac{m_V^4}{4\pi^2\alpha}\,\omega\,\mathrm{Im}\bar{A}_3(\nu, k^2)\,, \tag{4.4}$$

where $\bar{A}_3$ is the amplitude with the vector propagator taken out. Hence if νW_2 is to exhibit scaling behavior, $\mathrm{Im}\bar{A}_3$ must scale by itself. A standard even-signature Regge contribution to $\bar{A}_3$ will have the form

$$-\frac{\beta(t, k^2)}{\Gamma(\alpha(t))}\,\frac{1 + e^{-i\pi\alpha(t)}}{\sin\pi\alpha(t)}\left(\frac{2\nu}{\nu_0}\right)^{\alpha(t)-2}\,, \tag{4.5}$$

where the residue β and the scale factor ν_0 may in general depend on k^2. In order for $\mathrm{Im}\bar{A}_3(\nu, k^2)$ to show scaling behavior at low energies where the f and A_2 trajectories contribute in addition to the Pomeranchukon, each contribution of the form (4.5) must scale by itself. This conclusion is further supported by the observation that the difference between νW_2^p and νW_2^n, which is given by the A_2-exchange contribution, also scales. Since $\alpha(0) = 1$ for the Pomeranchukon and $\alpha(0) \approx \frac{1}{2}$ for the f and A_2, the simplest way in which to implement scaling behavior is to include a factor $(m_0^2 - k^2)^{2-\alpha(t)}$ for each Regge pole. This can be achieved either by assuming such a k^2 dependence for the residue function $\beta(t, k^2)$, or equivalently, by assuming a k^2-independent residue and taking the scaling parameter ν_0 to have the form

$$\nu_0 = m_0^2 - k^2\,.$$

In each case m_0^2 is a free parameter that sets the

Regge scale for $k^2=0$, but is unimportant for large $|k^2|$.

For each Regge exchange, therefore, we take

$$\beta(t)e^{-i\pi\alpha(t)/2}\left(\frac{2\nu}{m_0^2-k^2}\right)^{\alpha(t)-2}, \tag{4.6}$$

where we have introduced some simplifications that are valid for small $|t|$. Our model is in fact equivalent to the conventional scale-invariant Regge approach[10,12] for large $-k^2$ when the vector-meson propagator is taken into account in the full amplitude. As $s\to\infty$ at fixed k^2, Eq. (4.6) exhibits the standard Regge behavior $(s/\nu_0)^{\alpha(t)-2}$. The variable $\omega'=2\nu/(m_0^2-k^2)$ reduces to the usual scaling variable ω as $|k^2|\to\infty$, and at $k^2=0$ we have $\omega'=(s-m^2)/m_0^2$. The mass m_0^2 thus determines the Regge scale for real photons and contributes to the electroproduction scale-invariance breaking for small $|k^2|$. The magnitude of m_0^2 is of some importance for the determination of the realm of applicability of Regge ideas to deep-inelastic electroproduction. In Regge models it is common practice to take a scale factor of about 1 GeV^2, which for photoproduction implies $m_0^2\simeq 1$ GeV^2. On the other hand, Close and Gunion[26] have suggested $m_0\approx 0.22$ GeV, which implies that Regge behavior for inelastic electroproduction sets in only for large values of ω. At $k^2=0$, $E^\gamma_{\rm lab}=\omega m_0^2/2m$ so that $\omega=10$ corresponds to $E^\gamma_{\rm lab}\simeq 0.26$ GeV which is in the first resonance region. For $m_0=1$ GeV, the corresponding result is $E^\gamma_{\rm lab}\simeq 5.3$ GeV, and Regge poles might reasonably be expected to dominate. The relevance of this comparison is not clear, however. Since the electroproduction data we consider are for c.m. energies $W\geq 2$ GeV, we might expect Regge behavior for all k^2 and ω. This is certainly the case if we fix the Regge scale at 1 GeV say, and absorb the $(m_0^2-k^2)^{2-\alpha(t)}$ factor into the residue function, for then $\cos\theta_t$ is effectively asymptotic for all k^2. The ambiguity in the region of applicability of Regge poles to inelastic electroproduction is similar to the well-known problem in VMD of the meaning of the constraint $s+t+u=\sum m_i^2$ for variable mass. It is not clear *a priori* what variable is to be considered as fixed for the comparisons at different k^2. In the present case we presume that t must be fixed since we consider the forward direction both on and off shell. The question about the onset of Regge dynamics is basically a question of whether ω, ν, or s is to be held constant. This can best be settled by physical considerations. Duality for instance would suggest that the Regge explanation is valid above the region of prominent resonances, i.e., above $W\simeq 2$ GeV, and this could be taken to mean that we should consider fixed s for comparisons at different values of k^2. In our data fitting we treat m_0 as a free parameter and find that in general $m_0\simeq 1$ GeV is preferred. We shall return to this point in our discussion of the fit to the data in Sec. V. The large value of m_0 lends support to the hypothesis of Regge dominance for all ω in the scaling limit.

In our approach to inelastic electroproduction, the k^2 dependence of the Regge term (4.6) is in fact the off-shell mass dependence of the elastic vector-meson scattering amplitude. If Eq. (4.6) describes this process for all k^2, then the Pomeranchukon contribution has a zero at $k^2=m_0^2\approx 1$ GeV^2, and the other Regge poles have corresponding branch points. Asymptotically, $\sigma_{VN}\sim k^2$ as $|k^2|\to\infty$, since we know that the total amplitude $\sim 1/k^2$ as $k^2\to-\infty$. It should be pointed out, however, that we have no *a priori* knowledge of this k^2 dependence, and the form (4.6) is only that suggested by the spacelike k^2 data. We have no reason to expect the same form to be valid in the timelike region, where the only information we have is of the existence of the vector-meson poles, and these have been explicitly included in the total amplitude. In our phenomenological approach, any additional k^2 dependence must be determined by the data. The most direct way of investigating the timelike k^2 region is given by the photoproduction of electron or muon pairs, which does not involve the crossing necessary for comparison with e^+e^- annihilation experiments. The only experiments to date have concentrated on the ρ region, and it is of some interest that the cross section for vector-meson photoproduction is lower than that predicted by conventional VMD.[27] This could be interpreted as evidence for a k^2 dependence similar to that given by Eq. (4.6), and together with the measured total VN cross sections, it should be possible to make some more detailed comment on the possible timelike k^2 variation. However, this question is more appropriate to the detailed application of our model to vector-meson photoproduction, which we do not undertake here.

C. Threshold Behavior

One of the most striking features of the SLAC results is the rapid decrease of $\nu W_2/m^2$ as $\omega\to 1$. From Eq. (2.7) we see that $\omega\to 1$ corresponds to $s\to m^2$, or to the limit of elastic ep scattering. The kinematics of our model are those of elastic "γ" N scattering, and the $\gamma N\bar{N}$ vertex is not a limit of this process. Consequently we do not get this threshold behavior automatically.

It has been argued[6,8,28] that the threshold behavior of $W_{1,2}$ as $\omega\to 1$ is related to the large $-k^2$ behavior of the elastic form factors. In particular, if the form factor $G(k^2)\sim 1/k^4$ as $|k^2|\to\infty$, then $W_i\sim(\omega-1)^3$ as $\omega\to 1$. We take this effect into ac-

count by including a factor suggested by Moffat and Snell[12]:

$$\left(\frac{\omega^2-1}{\omega^2+\omega_0^2}\right)^3, \tag{4.7}$$

which $\sim(\omega-1)^3$ as $\omega\to 1$. The parameter ω_0 is determined by the fit to W_i for small ω.

Although this threshold behavior has to be imposed by hand on a simple Regge model, it is interesting to observe that from Eq. (4.6) for large $|k^2|$ each Regge pole $\sim\omega^{\alpha-2}$. Thus as $\omega\to 1$, all values of α enter. As we go to threshold we would expect the daughter trajectories to be just as important as the leading terms considered at larger values of ω. In this way we can interpret the threshold behavior in a Regge model as a result of the interference of the infinite sequence of daughter poles. Furthermore, there is no reason to suppose that the even G-parity daughters (P, f) behave in the same way as those of odd G-parity (A_2), so the threshold behavior of the deuterium to hydrogen ratio for electroproduction can be quite different from the low-energy behavior of the ratio $\sigma^{\gamma n}/\sigma^{\gamma p}$ for real photons.

Since we are using a phenomenological Regge model which includes leading singularities only, we do not have a prescription for the sequence of daughter trajectories, and the required threshold behavior must be imposed by hand. This is easily achieved by a factor such as the expression (4.7), but by itself this does not allow for differences between the f and A_2 daughter structure. The difference between $\sigma^{\gamma p}$ and $\sigma^{\gamma n}$ indicates a small A_2 contribution, whereas the inelastic electroproduction ratio $(D/H-1)<0.4$ for small ω requires a considerably larger admixture of isovector exchange. Thus we expect different daughter effects for the f and A_2. In order to allow for this in our phenomenological parametrization, we include the first daughter of the A_2. The possible importance of nonleading trajectories in deep-inelastic electroproduction has been suggested by Close and Gunion[26] in a slightly different context. In our approach the importance of nonleading trajectories is a direct consequence of our assumption of Regge behavior for small ω.

D. Model for the Invariant Amplitudes

We can summarize these various considerations in our model for the invariant amplitudes. If we neglect the small unnatural-parity contributions and assume leading order s-channel helicity conservation, only A_3 survives. Our Regge vector-dominance model then gives

$$A_3=-\left(\frac{\omega^2-1}{\omega^2+\omega_0^2}\right)^3\left(\frac{m_\rho^2}{m_0^2-k^2}\right)^2 \times\sum_i \beta_i e^{b_i t} e^{-i\pi\alpha_i(t)/2}\left(\frac{2\nu}{m_0^2-k^2}\right)^{\alpha_i(t)-2}, \tag{4.8}$$

where the sum is over the P, f, A_2, and A_2' trajectories, and the factor $\exp(b_i t)$ allows for some t dependence in the Regge residues. We use the Regge trajectories

$$\begin{aligned}\alpha_P(t)&=1+0.5t,\\ \alpha_f(t)&=0.5+0.9t,\\ \alpha_{A_2}(t)&=0.3+0.9t,\\ \alpha_{A_2'}(t)&=\alpha_{A_2}(t)-1.\end{aligned} \tag{4.9}$$

The P and f trajectories and the A_2 slope were fixed from fits to other reactions. The intercept of the A_2 trajectory is somewhat less well determined. For example, in a recent fit to the total photoabsorption cross section[29] it was found that the effective f-A_2 intercept could vary between $0.2\leq\alpha_{\rm eff}\leq 0.6$. Thus the σ_T^γ data are not sensitive to $\alpha_{A_2}(0)$, but the discussion of the electroproduction D/H ratio at small ω given above suggests that this ratio is more sensitive to this parameter. Because of possible daughter effects, however, $\alpha_{A_2}(0)$ is still not well determined. In our fits we treated the A_2-A_2' combination as an effective parametrization of the more complex situation, and allowed $\alpha_{A_2}(0)$ to vary over a limited range. The result $\alpha_{A_2}(0)=0.3$ is not necessarily the best value, but it does lead to acceptable fits to the available data.

Since the Pomeranchukon couples to a double-helicity-flip amplitude in the t channel, there must be a nonsense wrong-signature fixed pole at $t=0$ to prevent the Pomeranchukon from decoupling in the forward direction. General theoretical considerations[30] show that this fixed pole is allowed, and we assume that it is present. The possibility of a right-signature fixed pole at $J=0$ has been suggested on the basis of sum-rule analyses,[31] and the form of this pole for $k^2<0$ has been investigated.[26,32] Since this is a small effect, however, it is unlikely to be significant for data fitting, and we do not consider fixed poles further at present.

The electroproduction structure functions for nonasymptotic values of k^2 are given by Eqs. (4.1) and (4.2). In the scaling limit these expressions simplify to

$$\frac{\nu}{m^2}W_2=\frac{m_\rho^4}{4\pi^2\alpha}\left(\frac{\omega^2-1}{\omega^2+\omega_0^2}\right)^3 \times(\beta_P+\bar\beta_f\omega^{\alpha_f-1}\pm\bar\beta_{A_2}\omega^{\alpha_{A2}-1}\pm\bar\beta_{A_2'}\omega^{\alpha_{A2}-2}), \tag{4.10}$$

$$2W_1=\omega\left(\frac{\nu}{m^2}W_2\right), \tag{4.11}$$

where $\bar\beta_i=\beta_i\sin(\frac{1}{2}\pi\alpha_i)$, and the $\pm$ signs refer to

proton and neutron targets, respectively.

For simplicity in the fit to the Compton scattering differential cross section we assumed that the f and A_2 residues were constant, but we did allow an exponential t dependence in the Pomeranchukon residue. The fitted values of the parameters are

$$\begin{aligned} &\beta_P = 0.25\ \text{GeV}^{-4}, \quad \beta_f = 0.23\ \text{GeV}^{-4}, \\ &\beta_{A_2} = 0.075\ \text{GeV}^{-4}, \quad \beta_{A_2'} = -0.23\ \text{GeV}^{-4}, \\ &b_P = 1.76\ \text{GeV}^{-2}, \quad m_0 = 1.0\ \text{GeV}, \\ &\omega_0 = 0.8. \end{aligned} \tag{4.12}$$

The mass in the vector propagator was fixed to $m_\rho = 0.765$ GeV. The fits to the data are discussed in Sec. V.

V. THE FIT TO THE DATA

A. Photoabsorption Cross Section

There have been several experiments measuring the total absorption cross section for photons on both protons and neutrons.[33,34] In addition, Bloom *et al.*[35] have given values for $\sigma_T^{\gamma p}$ from the extrapolation of electroproduction cross sections to $k^2 = 0$. We included all this data in our fits, and in Fig. 1 we give the fit to both the proton and neutron photoabsorption cross sections. For clarity we have plotted the data of Ref. 33 only. The accurate data of Armstrong *et al.*[34] extend only to $E^\gamma \simeq 4.2$ GeV, and are consistent with the other data in this energy range. Unfortunately the higher-energy data are not very accurate, and considerable flexibility is possible in the fitted parameters.[29] The situation is worse for the neutron data, and the A_2-exchange contribution is not fixed with any accuracy. Nevertheless, in conjunction with the electroproduction data, $\sigma_T^{\gamma n}$ provides a useful constraint on the possible form of the A_2 daughter sequence.

The lack of marked energy dependence in σ_T^γ for $E^\gamma > 6$ GeV indicates Pomeranchukon dominance of the imaginary part of the forward amplitude. In our fit by $E^\gamma \simeq 20$ GeV, σ_T^γ is within a few microbarns of its asymptotic value. The cross-section data alone can be fitted over a range of the parameters, but Pomeranchukon dominance is characteristic of any such fit. This has important implications for the large ω behavior of νW_2.

B. The Compton Differential Cross Section

There are now good Compton differential cross-section data available over a wide range of energies.[36] In the forward direction these data are consistent with σ_T^γ and the optical theorem, so they do not provide significant additional constraints on the magnitude of the residues. The differential cross section serves to determine the t dependence of the residues, however, and we found good fits with an exponential factor in the Pomeranchukon residue only.

Our fit to the data of Ref. 36 is shown in Fig. 2. The model predicts a slight shrinkage as is expected from a model without cut effects, and the

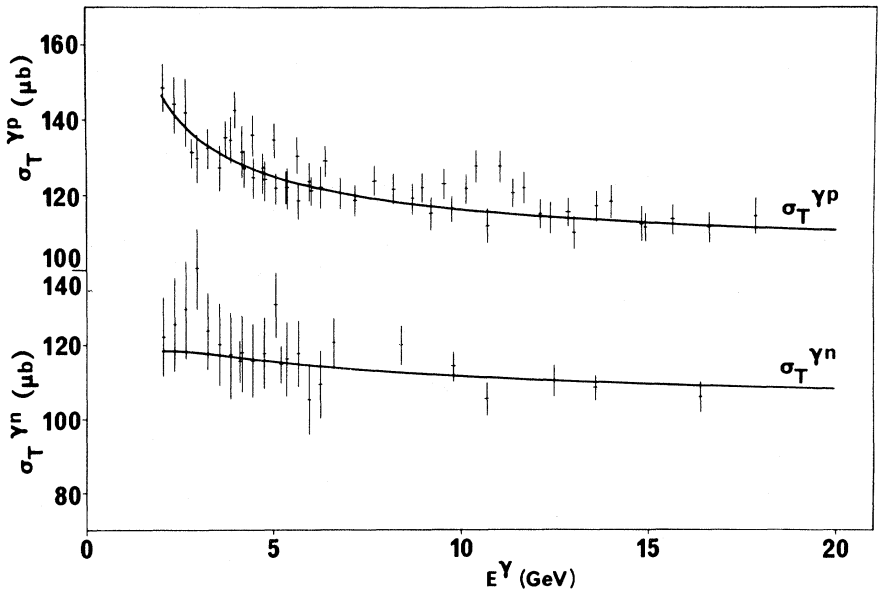

FIG. 1. The fit to the total photoabsorption cross section for $E^\gamma > 2$ GeV. The data are taken from Ref. 33. Notice the different scales for the proton and neutron data.

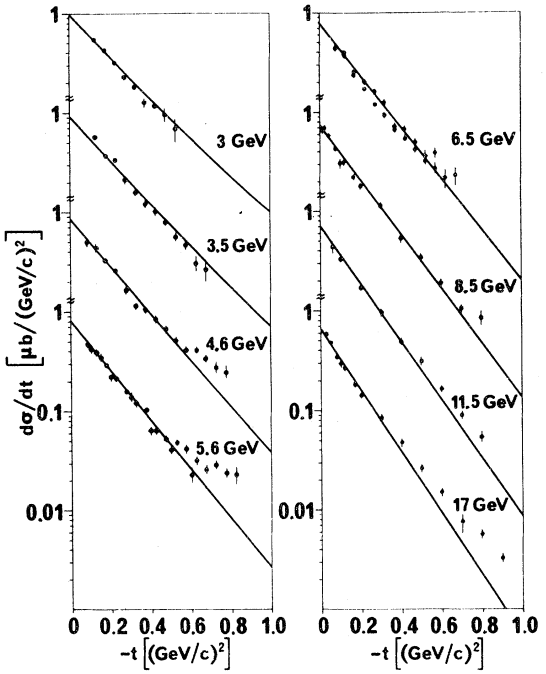

FIG. 2. The Compton differential cross section between 3 and 17 GeV. The data are taken from Ref. 36. Where data from different experiments differ only slightly in energy they have been plotted together, and the central energy quoted.

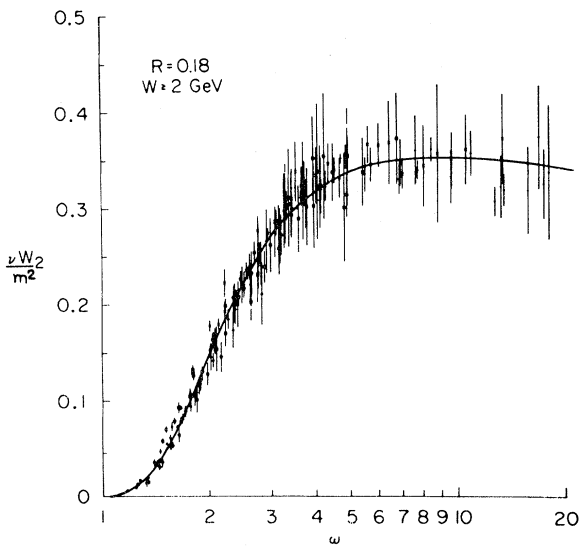

FIG. 3. The scaling-limit curve for $\nu W_2/m^2$ from our model plotted against data from Ref. 2 with $W \geq 2$ GeV and $R = 0.18$. Only points for $-k^2 > 1$ (GeV/c)^2 are shown.

fit to the wider angle data at high energies is not perfect. Some improvement would be possible with a P residue of the form $\exp(bt + ct^2)$, but in the interests of simplicity we did not include a quadratic term. The over-all fit is good, and provides further justification for our assumption that Compton scattering is dominated by the invariant amplitude A_3, since if the other amplitudes were present, they might be expected to become relatively more important as $|t|$ increases.

C. Inelastic Electroproduction Structure Functions

Our fits to the inelastic electroproduction structure function $\nu W_2/m^2$ is shown in Fig. 3. Some comment is necessary to explain the exact significance of this fit. In order to determine the parameters of our model as reliably as possible, we fitted the structure functions $\nu W_2/m^2$ calculated from the electroproduction cross sections of Ref. 2 using the ratio $R = \sigma_L/\sigma_T = -m^2k^2/\nu^2$ rather than the more usual constant value of $R = 0.18$. As we demonstrated in Sec. III, the variable R of Eq. (3.16) is a natural feature of our model, and is quite consistent with the direct determination of R from experiment.[2] In Fig. 3, however, we plot our result against the data for $R = 0.18$ in order to facilitate comparison with other models. The difference between these data and those we actually fitted is slight, except for the larger values of ω where $R = -m^2k^2/\nu^2$ gives a value of $\nu W_2/m^2$ approximately 5% smaller. Thus the fit is slightly better than is indicated by the figure.

We used data for $W \geq 2$ GeV and $-k^2 \geq 1$ (GeV/c)^2 only, and fitted with the exact expression (4.8) rather than the scaling limit form of Eq. (4.10). The smooth curve plotted is, however, the result for $k^2 = -\infty$. For $-k^2 > 1$ (GeV/c)^2, the scaling curve differs only marginally from the exact form, as we shall see when we discuss scale-invariance breaking. Since our model predicts $R = -m^2k^2/\nu^2$, W_1 also scales, and we have $2W_1 = \omega(\nu W_2/m^2)$. This relation is perfectly consistent with the available data, so the fit to W_1 does not add anything new, and we will not consider W_1 further.

Several important features emerge in the present model. Firstly, our fit to νW_2 is Pomeranchukon dominated for $\omega > 10$. Thus we would agree with Harari's[10] suggestion that deep-inelastic electroproduction is primarily diffractive and not with models[8,11,26] which suggest that a large part of the cross section is nondiffractive in origin. Only experiment can determine whether the present model is correct. We predict that by $\omega \simeq 20$, $\nu W_2/m^2$ has essentially reached its constant limit, and at $\omega = 100$ it has fallen only to $\nu W_2/m^2 \simeq 0.31$. The scanty data for $\omega > 20$ appears to indicate a smaller asymptotic limit, but these values of ω are attained only for $-k^2 < 0.8$ (GeV/c)^2, and Eq. (4.2) clearly demonstrates the kinematic suppression of νW_2 for small $|k^2|$ related to the fact that νW_2 must vanish

at $k^2=0$ [Eq. (2.10]. It is unwise to fit the scaling limit curve to such data, and we suggest that the leveling of $\nu W_2/m^2$ for $\omega>5$ is strongly indicative of Pomeranchukon dominance. At least the data are consistent with this model, and there are not enough points to fit only for $\omega>12$, say.[26]

We further remark that the relative normalization of σ_T^γ and νW_2 in our model is determined by the Regge scale parameter m_0 and the vector-meson mass m_V of the propagator (4.3). Asymptotically,

$$\sigma_T^\gamma = 389.39 m_0^2 \beta_P \ \mu\text{b} \tag{5.1}$$

and

$$\frac{\nu}{m^2} W_2 = \frac{m_V^4}{4\pi^2\alpha}\beta_P . \tag{5.2}$$

Although m_V was fixed to $m_\rho = 0.765$ GeV in the final fit, we tested the dependence of the result on m_V by doing an independent fit with m_V as a parameter. From a wide range of starting values for both m_0 and m_V, the values (4.12) were always reproduced with m_V changing to perhaps 0.78 GeV, and m_0 correspondingly slightly above 1 GeV. It seemed reasonable, therefore, to fix these parameters at their quoted values.

The nonleading A_2' trajectory is unimportant in the fit to νW_2 and σ_T^γ. Its absence would be readily accommodated by a slight adjustment of the other residues. Its importance is felt only for the fit to the neutron to proton ratio discussed in Sec. V D. In this connection we refer to the discussion of small ω behavior in Sec. IV C. Since we perform our k^2 continuation at fixed s and t, we expect Regge behavior down to threshold in the scaling limit. The fact that $m_0 = 1$ GeV is preferred by our fit lends further support to this idea. We suggest that the observed $(\omega-1)^3$ threshold behavior is in fact the effect of lower-lying trajectories that become important as $\omega \to 1$. Since we have imposed this threshold behavior by hand, the effective A_2-A_2' complex serves only to distinguish different isospin exchanges, and does not affect this behavior. The detailed interpretation of the threshold behavior is unfortunately outside the scope of our simple model, and we merely note that our phenomenological expression (4.7) works perfectly.

The present model suggests a rather different interpretation of the data to that proposed by Bloom and Gilman.[8] For moderate values of $|k^2|$, $W<2$ GeV corresponds to small ω, and the fact that the scaling limit curve for large W averages the resonances for small W does not have an obvious interpretation in terms of duality. The importance of low-lying trajectories for small ω can completely mask the Pomeranchukon-background, nondiffractive-resonance duality, since these lower trajectories must interfere with the Pomeranchukon in order to produce the correct threshold behavior. The Rittenberg and Rubinstein[9] scaling variable $\omega_W = (2\nu + M^2)/(m_0^2 - k^2)$ may be significant for the dual interpretation of the present approach, however, since this is just the variable needed to prevent the daughter series from diverging at threshold for $k^2=0$. For $M=m_0$, the threshold behavior of the extrapolated Regge terms in Compton scattering is precisely that of νW_2. In any case, the importance of low-lying trajectories even for high energies occasioned by the k^2 dependence in inelastic electroproduction obscures the simple Harari-Freund[37] dual interpretation.

D. The Neutron to Proton Ratio

Much of the difficulty in the interpretation of the electroproduction data stems from the observed small ratio of the cross section off neutrons to that off protons at small ω. The data[2] are shown in Fig. 4, and a reasonable extrapolation would give $R' \equiv (D/H - 1)(\omega=1) \simeq 0.3$. If we ignore the A_2' contribution, a Regge fit to σ_T^γ would predict $R'(\omega=1) \simeq 0.74$, whereas with an effective A_2' trajectory, our model gives $R'(\omega=1) \simeq 0.26$. The data from Ref. 2 are not corrected for deuterium effects, and we simply fitted the data as shown with the full expression for W_2^n/W_2^p. In Fig. 4 we have plotted the scaling limit curve, and find satisfactory agreement with the data. Certainly, a reasonable fit for $\omega<4$ is impossible without the A_2' contribution. Any attempt at such a fit forces a considerably different interpretation on the rest of the data. In the absence of an A_2', the ratio for small ω can be lowered only by reducing the P and f terms in inelastic electroproduction, and to maintain the fit to the Compton data, we must reduce both m_0 and m_V. This obscures the meaning

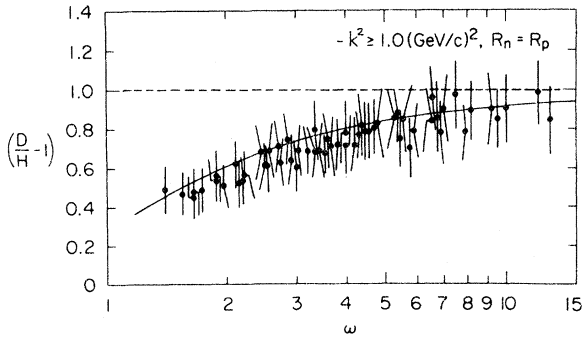

FIG. 4. The fit to the neutron to proton ratio. The data from Ref. 2 have not been corrected for deuterium effects.

of a Regge fit for small ω, and the over-all quality of the fit is considerably reduced.

E. Scale-Invariance Breaking

In Fig. 5 we plot our model predictions for $\nu W_2/m^2$ at small $|k^2|$ and fixed ω. The data are taken from Ref. 2 with the fixed value of $\sigma_L/\sigma_T = 0.18$. Since νW_2 is constrained to vanish at $k^2 = 0$, the data must show deviations from scaling behavior for small $|k^2|$. We can see from Fig. 5 that our model describes this fall off for $|k^2| < 1$ $(\mathrm{GeV}/c)^2$ very well. It should be pointed out that at no stage of our fitting procedure did we actually fit this data, so the curves of Fig. 5 represent an absolute prediction of our model in terms of the parameters determined by the fit to the other data.

It is interesting to observe that the model predicts approximate scaling to lower values of $|k^2|$ for small ω. This should not be taken too seriously, because for fixed ω, small $|k^2|$ corresponds to small W, and for $\omega = 5$ for instance, $W = 2$ GeV for $k^2 \simeq -0.8$ $(\mathrm{GeV}/c)^2$. Nonleading effects become important for small $|k^2|$ and ω, and a Regge model is unreliable below $|k^2| \simeq 0.8$ $(\mathrm{GeV}/c)^2$ in Fig. 5(a). It is important to notice, however, that the scale-invariance breaking is not necessarily characterized by a small mass. In our model the scale breaking depends on $m_0 = 1$ GeV and $m_\rho = 0.765$ GeV. In spite of this, we essentially reach the scaling limit by $k^2 \simeq -1$ $(\mathrm{GeV}/c)^2$.

VI. DISCUSSION

The excellent fits that we have obtained clearly demonstrate that the elastic scattering of both real and virtual photons from nucleons can be understood in terms of the same dynamical model. An important feature of the model is the inclusion of the vector-meson propagator to describe the factorizable k^2 dependence of the virtual photon. This provides a connection between the low k^2 region where conventional VMD is expected to be reliable, and a scale-invariant Regge model for the large spacelike k^2 region. By requiring that the continuation to $k^2 = 0$ from spacelike values of k^2 be smooth, we have been able to relate deep-inelastic electroproduction to Compton scattering. Since the continuation is specified in terms of invariant amplitudes, there is no ambiguity associated with the Lorentz frame dependence of the longitudinal-transverse decomposition of the virtual photon. In order to make definite predictions, it is necessary to make the further assumptions of minimal k^2 dependence of the invariant amplitudes and leading-order s-channel helicity conservation for Compton scattering. These are reasonable assumptions, and they lead directly to the prediction $\sigma_L/\sigma_T = -m^2k^2/\nu^2$. This prediction is a central feature of our model, and highlights the difference between our formulation of VMD and the more usual approach of Sakurai.[1] The assump-

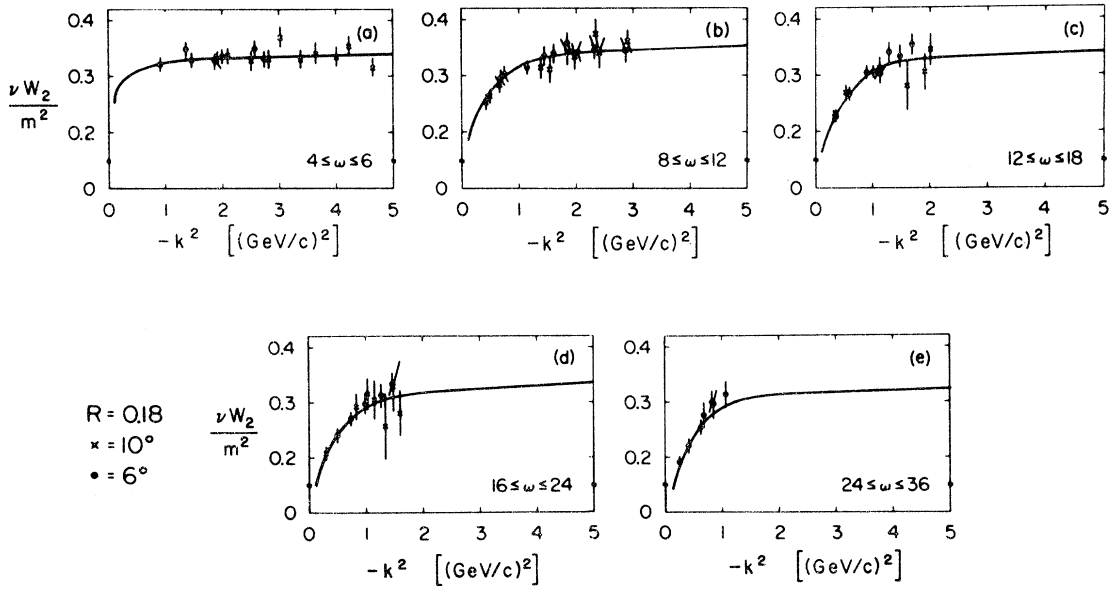

FIG. 5. The plot of $\nu W_2/m^2$ against $|k^2|$ for various values of ω. The data are again taken from Ref. 2, and illustrate the scale-invariance breaking for small $|k^2|$ predicted by our model.

tion of minimal k^2 dependence is also supported by the data, since terms of $O(k^4)$ in the C_i would destroy the scale invariance of the model.

It should be pointed out that our model requires the invariant amplitudes to be Reggeized directly or via the singularity-free t-channel helicity amplitudes. If we Reggeize the forward s-channel helicity amplitude for Compton scattering $f^{\gamma}_{1\frac{1}{2},1\frac{1}{2}} + f^{\gamma}_{1-\frac{1}{2},1-\frac{1}{2}}$, the transformation to the invariant amplitudes necessary for the k^2 continuation introduces a factor $1/(s-m^2)^2$. It is easy to verify that in this case νW_2 will scale only if the vector propagator is absent. We get instead a factor

$$\frac{\nu^2}{(s-m^2)^2} = \frac{1}{4}\left(\frac{\omega}{\omega-1}\right)^2$$

which diverges at threshold, but can readily be accommodated by modifying the phenomenological threshold factor (4.7). This gives a model very similar to that of Moffat and Snell.[12] We consider such an approach to be somewhat artificial, however. After all, Regge poles are t-channel objects, and since the forward t-channel helicity amplitude has double helicity flip, it is characterized by the $\nu^{\alpha-2}$ behavior of the invariant amplitude A_3. The forward s-channel helicity amplitude $\sim\nu^{\alpha}$, but it has double zero at $s=m^2$. This singularity is unimportant for large s, but in principle it should be removed, especially if one wishes to look at the amplitude near threshold. The k^2 continuation singles out the invariant amplitudes as the basic dynamical objects, and Regge theory tells us that these should be parametrized via t-channel helicity amplitudes. Our direct parametrization of A_3 is entirely equivalent to the t-channel approach, but not to the s-channel parametrization. Since the incorporation of VMD is a basic feature of our model, it is of some importance that this distinction between the s- and t-channels be understood.

Our approach to the data is of necessity phenomenological, but we feel that by taking scaling behavior as a fact to be understood rather than predicted, our detailed fit to the data leads to some new understanding of deep-inelastic electroproduction. In the first place our model demonstrates that inelastic electroproduction for large $|k^2|$ is consistent with the Compton data at $k^2=0$ within the framework of vector-meson dominance of the electromagnetic current. We use the same simple generalization of VMD that has been successfully applied to other processes,[15] and it is of some interest that we find that the additional k^2 dependence of the off-shell vector-meson scattering amplitude necessary in the presence of the vector propagator is simply given by replacing the energy variable ν/ν_0 by ω as in conventional scale-invariant Regge models. Since our amplitude has the explicit vector-meson poles, it would be possible to study vector-meson photoproduction, electroproduction, and vector-meson-nucleon scattering by taking the residues of these poles. To investigate these processes, however, the kinematical analysis must be extended to include the extra amplitudes present for inelastic scattering.

There has been some interest recently[38] in the k^2 dependence of the diffraction slope which can be studied in vector-meson electroproduction. This has bearing on the question of the size of the photon in the spacelike region, and since the photon interacts with hadrons via an off-shell vector meson in our model, we would not expect the rapid onset of pointlike behavior. The experimental situation of ρ^0 electroproduction is not clear,[39] and the question of whether the interaction radius changes with k^2 has not been resolved. Although our present kinematical analysis does not allow us to consider ρ^0 electroproduction, we can investigate elastic virtual Compton scattering where $k^2 = k'^2 < 0$. This process is not experimentally accessible, but it is in fact a more direct measure of the interaction radius than ρ^0 electroproduction since both photons are off shell.[40] With our model amplitude, and the parameters determined in the fit described above, it is straightforward to predict the differential cross section for "γ" $p \to$ "γ"p, where "γ" is a spacelike photon. In Fig. 6 we plot our predictions for this reaction at a fixed value of $\nu = 6$ GeV^2 and $0 \leq |k^2| \leq 5$ (GeV/c)^2. The diffrac-

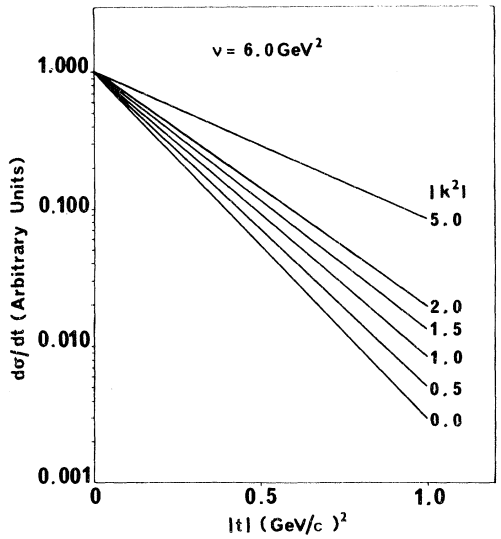

FIG. 6. Differential cross section for virtual Compton scattering "γ"$p \to$ "γ"p. The variable k^2 is given in units of (GeV/c)^2, and in order to display the change in slope, the inessential k^2 dependence of the forward cross section has been divided out.

tion slope changes by more than a factor of 2 in this range, from $\exp(6t)$ at $k^2=0$ to $\exp(2.5t)$ at $k^2=-5$. At fixed ν the main effect comes from the Regge shrinkage, since $2\nu/(m_0^2-k^2)$ decreases as $|k^2|$ increases, but a similar change in the slope is observed if we plot $d\sigma/dt$ for fixed W. For very large c.m. energies, the k^2 dependence arising from the nonleading amplitudes becomes unimportant, but the effect persists at fixed ν or fixed W simply because of this Regge shrinkage. Thus a change in the diffraction slope of the order of that shown in Fig. 6 can be simply interpreted in terms of the well-known fact that for Regge poles at fixed k^2, the radius of the interaction increases as the energy increases. Similar considerations will clearly apply to the observable ρ^0 electroproduction process.

Other interesting features of our model are the prediction of Pomeranchukon dominance of $\nu W_2(\omega)$, and the possible importance of nonleading Regge trajectories for small ω. These predictions are most easily tested by accurate high-energy photoabsorption cross sections for both protons and neutrons, and more directly by the measurement of νW_2 for large ω and $|k^2|>1$ (GeV/c)^2. If νW_2 remains approximately constant above $\omega\simeq 6$, then it would seem that the scaling region is predominantly diffractive, and current duality arguments may require reformulation.

ACKNOWLEDGMENTS

It is a pleasure to thank Professor A. Donnachie for his helpful interest in this work and for a critical reading of the manuscript. The use of the computing facilities at Daresbury Nuclear Physics Laboratory is also gratefully acknowledged.

APPENDIX

We use units such that $\hbar=c=1$, and our metric is $g_{00}=-g_{ii}=1$ so that k^2 is negative for spacelike momenta. States are normalized by

$$\langle\vec{p}'|\vec{p}\rangle=2E(2\pi)^3\delta^{(3)}(\vec{p}'-\vec{p}), \tag{A1}$$

and spinors are normalized to $\bar{u}u=2m$.

Invariant amplitudes are defined in terms of the T matrix

$$T=\bar{u}(p')M_{\lambda\mu}\epsilon^{\lambda}(k)\epsilon^{\mu}(k')u(p)$$

by

$$M\equiv M_{\lambda\mu}\epsilon^{\lambda}\epsilon^{\mu}=\sum_i K_iC_i\ . \tag{A2}$$

The amplitudes for virtual-photon elastic scattering are defined in Eq. (3.2), and the two redundant covariants are eliminated by the equivalence theorems

$$(P_\lambda k_\mu+k'_\lambda P_\mu)\not{Q}=mK_4+\nu K_8-2mK_9+m\nu K_{11}+P^2K_{12}, \tag{A3}$$

$$mk'_\lambda k_\mu\not{Q}=(\nu+\tfrac{1}{4}t)K_3+(\nu-Q^2)K_4+mQ^2K_8-2\nu K_9-\tfrac{1}{4}tK_{10}+(\nu^2+\tfrac{1}{4}tQ^2)K_{11}+m\nu K_{12}. \tag{A4}$$

Similarly, the invariant amplitudes for on-shell Compton scattering are defined in Eq. (3.3) by

$$M=\sum_{i=1}^{6}K_i^{\gamma}A_i\ . \tag{A5}$$

Again there are two equivalence theorems which read

$$2m^2(k\cdot k'g_{\lambda\mu}-k'_\lambda k_\mu)\not{Q}=2m\nu K_1^{\gamma}-\tfrac{1}{4}mtK_5^{\gamma}+\nu K_6^{\gamma}, \tag{A6}$$

$$2m[k\cdot k'(P_\lambda\not{Q}\gamma_\mu+\gamma_\lambda\not{Q}P_\mu)-\nu(k'_\lambda\not{Q}\gamma_\mu+\gamma_\lambda\not{Q}k_\mu)+2\nu g_{\lambda\mu}(m\not{Q}-\nu)-\tfrac{1}{2}\not{k}\not{k}'(P_\lambda k_\mu+k'_\lambda P_\mu)+\nu k'_\lambda k_\mu]=m\nu K_5^{\gamma}+P^2K_6^{\gamma}. \tag{A7}$$

Notice that for Compton scattering we get additional relations like

$$\gamma_5\epsilon_{\lambda\mu\alpha\beta}k^{\alpha}k'^{\beta}=\frac{1}{2m}K_6^{\gamma}. \tag{A8}$$

It is straightforward but tedious to derive the relations between the invariant and helicity amplitudes. Since we need these expressions for our work, we give them here in full. For these relations we use the slightly different notation $K_\mu=(k_0,\vec{k})$ for the virtual-photon four-momentum, and put $k\equiv|\vec{k}|$. The c.m. nucleon energy is E, and

$$E=\frac{s+m^2-K^2}{2W}\,,$$

$$k_0=\frac{s-m^2+K^2}{2W}\,,$$

$$4sk^2=[K^2-(W+m)^2][K^2-(W-m)^2]\,,$$

where $s\equiv W^2$, and m is the nucleon mass.

The s-channel helicity amplitudes for the elastic scattering of virtual photons on nucleons are

$$\begin{aligned}f_{0\frac12,0\frac12}=\frac{2\cos(\frac12\theta)}{|K^2|}\{&k^2[E+k_0\cos^2(\tfrac12\theta)]^2[mC_1+(k^2+Ek_0)C_2]+4mk^2k_0{}^2\sin^4(\tfrac12\theta)(C_3-C_4-C_9+2C_{10})\\&+(k^2-k_0{}^2\cos\theta)[mC_5+(k^2+Ek_0)C_6]\\&+4mk^2k_0W\sin^2(\tfrac12\theta)(C_4+C_9)+2k^2W[E+k_0\cos^2(\tfrac12\theta)]C_7\\&+4k^2k_0W\sin^2(\tfrac12\theta)C_8+4mk_0{}^2\sin^2(\tfrac12\theta)C_{11}-4K^2k_0E\sin^2(\tfrac12\theta)C_{12}\}\,,\end{aligned}$$

$$\begin{aligned}f_{0\frac12,0-\frac12}=-\frac{2\sin(\frac12\theta)}{|K^2|}\{&k^2[E+k_0\cos^2(\tfrac12\theta)]^2(EC_1+mk_0C_2)+4k^2k_0{}^2E\sin^4(\tfrac12\theta)(C_3-C_4-C_9+2C_{10})\\&+(k^2-k_0{}^2\cos\theta)(EC_5+mk_0C_6)+4k^2k_0WE\sin^2(\tfrac12\theta)(C_4+C_9)\\&+2mk^2[E+k_0\cos^2(\tfrac12\theta)]C_7+4mk^2k_0\sin^2(\tfrac12\theta)C_8-2k^2k_0W[E+k_0\cos^2(\tfrac12\theta)]C_9\\&-4k^2k_0{}^2W\sin^2(\tfrac12\theta)C_{10}-4k_0[k^2+Ek_0\cos^2(\tfrac12\theta)]C_{11}+4mK^2k_0\cos^2(\tfrac12\theta)C_{12}\}\,,\end{aligned}$$

$$f_{0\frac12,1\frac12}=f_{0-\frac12,1-\frac12}=-\frac{2\sqrt2\sin(\frac12\theta)}{(|K^2|)^{1/2}}\{k^2[E+k_0\cos^2(\tfrac12\theta)]C_7+2k^2k_0\sin^2(\tfrac12\theta)C_8+2mk_0C_{11}-2k_0[Ek_0+k^2\cos^2(\tfrac12\theta)]C_{12}\}\,,$$

$$\begin{aligned}f_{0-\frac12,1-\frac12}=\frac{\sqrt2\sin(\frac12\theta)}{(|K^2|)^{1/2}}\cos^2(\tfrac12\theta)\{&-k^2[E+k_0\cos^2(\tfrac12\theta)][mC_1+(k^2+Ek_0)C_2]+4mk^2k_0\sin^2(\tfrac12\theta)(C_3-C_4-C_9+2C_{10})\\&+2mk^2W(C_4+C_9)+2mk_0(C_5+2C_{11})+2k_0(k^2+Ek_0)(C_6-2C_{12})-k^2W(C_7-2C_8-2C_{12})\}\,,\end{aligned}$$

$$\begin{aligned}f_{0\frac12,1-\frac12}=\frac{\sqrt2\cos(\frac12\theta)}{(|K^2|)^{1/2}}\sin^2(\tfrac12\theta)\{&k^2[E+k_0\cos^2(\tfrac12\theta)](EC_1+mk_0C_2)-4k^2k_0E\sin^2(\tfrac12\theta)(C_3-C_4-C_9+2C_{10})\\&-2k^2EW(C_4+C_9)-2k_0E(C_5+2C_{11})-2mk_0{}^2(C_6-2C_{12})\\&+mk^2(C_7-2C_8-2C_{12})-k^2k_0W(C_9-2C_{10})\}\,,\end{aligned}\tag{A9}$$

$$f_{0-\frac12,1\frac12}=-f_{0\frac12,1-\frac12}+\frac{2\sqrt2\cos(\frac12\theta)}{(|K^2|)^{1/2}}[k^2k_0W\sin^2(\tfrac12\theta)(C_9-2C_{10})-k^2W^2C_9-2(k^2+Ek_0)C_{11}+2mK^2C_{12}],$$

$$f_{1\frac12,1\frac12}=f_{1-\frac12,1-\frac12}-4\cos(\tfrac12\theta)[k^2\sin^2(\tfrac12\theta)(C_7-2C_8-2C_{12})-2mC_{11}+2(k^2+Ek_0)C_{12}]\,,$$

$$\begin{aligned}f_{1-\frac12,1-\frac12}=-\cos^3(\tfrac12\theta)\{&k^2\sin^2(\tfrac12\theta)[mC_1+(k^2+Ek_0)C_2]+4mk^2\sin^2(\tfrac12\theta)(C_3-C_4-C_9+2C_{10})\\&+2m(C_5+2C_{11})+2(k^2+Ek_0)(C_6-2C_{12})\}\,,\end{aligned}$$

$$\begin{aligned}f_{1\frac12,1-\frac12}=\sin(\tfrac12\theta)\cos^2(\tfrac12\theta)[&k^2\sin^2(\tfrac12\theta)(EC_1+mk_0C_2)+4k^2E\sin^2(\tfrac12\theta)(C_3-C_4-C_9+2C_{10})\\&+2E(C_5+2C_{11})+2mk_0(C_6-2C_{12})+2k^2W(C_9-2C_{10})]\,,\end{aligned}$$

$$\begin{aligned}f_{1\frac12,-1\frac12}=\sin^2(\tfrac12\theta)\cos(\tfrac12\theta)\{&k^2\cos^2(\tfrac12\theta)[mC_1+(k^2+Ek_0)C_2]+4mk^2\cos^2(\tfrac12\theta)(C_3-C_4-C_9+2C_{10})\\&-2m(C_5+2C_{11})-2(k^2+Ek_0)(C_6-2C_{12})+2k^2(C_7-2C_8-2C_{12})\}\,,\end{aligned}$$

$$f_{1\frac12,-1-\frac12}=-f_{1-\frac12,-1\frac12}-4\sin(\tfrac12\theta)[k^2W\cos^2(\tfrac12\theta)(C_9-2C_{10})+2EC_{11}-2mk_0C_{12}]\,,$$

$$f_{1-\frac12,-1\frac12}=\sin^3(\tfrac12\theta)[k^2\cos^2(\tfrac12\theta)(EC_1+mk_0C_2)+4k^2E\cos^2(\tfrac12\theta)(C_3-C_4-C_9+2C_{10})-2E(C_5+2C_{11})-2mk_0(C_6-2C_{12})]\,.$$

The s-channel helicity amplitudes for on-shell Compton scattering are simpler, and with the same notation as before, but with $K^2=0$,

$$f^{\gamma}_{1\frac12,1\frac12}=-2k^2\cos(\tfrac12\theta)\{ms\cos^2(\tfrac12\theta)A_2+2[s-m^2\sin^2(\tfrac12\theta)]A_3-2[s+m^2\sin^2(\tfrac12\theta)]A_4\}\,,$$

$$f^{\gamma}_{1-\frac12,1-\frac12}=-2k^2s\cos^3(\tfrac12\theta)(mA_2+2A_3+2A_4)\,,$$

$$f^{\gamma}_{1\frac{1}{2},1-\frac{1}{2}} = 2k^2 W \sin(\tfrac{1}{2}\theta)\cos^2(\tfrac{1}{2}\theta)[EWA_2 + 2m(A_3 + A_4)] ,$$

$$f^{\gamma}_{1\frac{1}{2},-1\frac{1}{2}} = -4k^2 \sin^2(\tfrac{1}{2}\theta)\cos(\tfrac{1}{2}\theta)[m(A_1 + \tfrac{1}{2}P^2A_2 + mA_3 + 2A_5) + EWA_4] , \tag{A10}$$

$$f^{\gamma}_{1\frac{1}{2},-1-\frac{1}{2}} = 4k^2 \sin(\tfrac{1}{2}\theta)\{E \sin^2(\tfrac{1}{2}\theta)(A_1 + \tfrac{1}{2}P^2A_2 + mA_3) - W[2 - \sin^2(\tfrac{1}{2}\theta)](mA_4 + 2A_5) + mk \sin^2(\tfrac{1}{2}\theta)(A_4 + 2A_6)\} ,$$

$$f^{\gamma}_{1-\frac{1}{2},-1\frac{1}{2}} = -4k^2 \sin^3(\tfrac{1}{2}\theta)[E(A_1 + \tfrac{1}{2}p^2A_2 + mA_3) + m(EA_4 - 2kA_6) - 2(k - E)A_5] .$$

These relations are equivalent to those given by Jones and Scadron[20] for instance.

---

[1]J. J. Sakurai, Phys. Rev. Letters 22, 981 (1969); C. F. Cho, G. J. Gounaris, and J. J. Sakurai, Phys. Rev. 186, 1734 (1969); C. F. Cho and J. J. Sakurai, Phys. Letters 31B, 22 (1970).

[2]E. D. Bloom *et al.*, Phys. Rev. Letters 23, 930 (1969); M. Breidenbach *et al.*, *ibid.* 23, 935 (1969); E. D. Bloom *et al.*, in *Proceedings of the Fifteenth International Conference on High Energy Physics, Kiev, U.S.S.R., 1970* (Atomizdat, Moscow, 1971).

[3]See, for instance, F. J. Gilman and R. E. Taylor, in *Proceedings of the Fourth International Symposium on Electron and Photon Interactions at High Energies, Liverpool, 1969,* edited by D. W. Braben and R. E. Rand (Daresbury Nuclear Physics Laboratory, Daresbury, Lancashire, England, 1970); J. D. Bjorken, in Proceedings of the 1970 Scottish Universities' Summer School (Plenum, New York, to be published); C. H. Llewellyn Smith, CERN Report No. CERN-TH-1188, 1970 (unpublished); H. Harari, J. D. Bjorken, and H. Kendall, rapporteur's talks, in *Proceedings of the International Symposium on Electron and Photon Interactions at High Energies, 1971,* edited by N. B. Mistry (Cornell Univ. Press, Ithaca, N. Y., 1972).

[4]J. D. Bjorken, Phys. Rev. 179, 1547 (1969).

[5]R. P. Feynman, Phys. Rev. Letters 23, 1415 (1969); in *High Energy Collisions,* edited by C. N. Yang *et al.*, (Gordon and Breach, New York, 1969).

[6]J. D. Bjorken and E. Paschos, Phys. Rev. 185, 1975 (1969); S. D. Drell, D. J. Levy, and T.-M. Yan, Phys. Rev. Letters 22, 744 (1969); Phys. Rev. 187, 2159 (1969); Phys. Rev. D 1, 1035 (1970); 1, 1617 (1970); S. D. Drell and T.-M. Yan, Phys. Rev. Letters 24, 181 (1970); Phys. Rev. D 1, 2402 (1970); Ann. Phys. (N.Y.) 66, 578 (1971).

[7]M. Gourdin, in the 1971 Erice Lectures, CERN Report No. CERN-TH-1384, 1971 (unpublished); P. V. Landshoff, J. C. Polkinghorne, and R. D. Short, Nucl. Phys. B28, 225 (1971); P. V. Landshoff and J. C. Polkinghorne, *ibid.* B28, 240 (1971); B33, 221 (1971); B35, 642 (1971); Phys. Letters 34B, 621 (1971); K. G. Wilson, Phys. Rev. Letters 27, 690 (1971); C. W. Gardiner and D. P. Majumdar, Phys. Rev. D 2, 151 1970; 2, 2040 (1970).

[8]E. D. Bloom and F. J. Gilman, Phys. Rev. Letters 25, 1140 (1970); Phys. Rev. D 4, 2901 (1971).

[9]V. Rittenberg and H. R. Rubinstein, Phys. Letters 35B, 50 (1971); F. W. Brasse *et al.*, Nucl. Phys. B39, 421 (1972).

[10]H. D. I. Abarbanel, M. L. Goldberger, and S. B. Treiman, Phys. Rev. Letters 22, 500 (1969); R. A. Brandt, *ibid.* 22, 1149 (1969); H. Harari, *ibid.* 22, 1078 (1969); 24, 286 (1970); H. R. Pagels, Phys. Letters 34B, 299 (1971); Phys. Rev. D 3, 1217 (1971).

[11]P. V. Landshoff and J. C. Polkinghorne, Nucl. Phys. B19, 432 (1970); R. C. Brower, A. Rabl, and J. H. Weis, Nuovo Cimento 65A, 654 (1970).

[12]J. W. Moffat and V. G. Snell, Phys. Rev. D 3, 2848 (1971); 4, 1452 (1971).

[13]D. M. Ritson, Phys. Rev. D 3, 1267 (1971); K. Fujikawa, *ibid.* 4, 2794 (1971); J. J. Sakurai and D. Schildknecht, Phys. Letters 40B, 121 (1972); Ashok suri and D. R. Yennie, Ann. Phys. (N.Y.) 72, 243 (1972); S. J. Brodsky, F. E. Close, and J. F. Gunion, Phys. Rev. D 6, 177 (1972).

[14]N. N. Achasov and G. N. Shestakov, Yad. Fiz. 11, 1090 (1970) [Sov. J. Nucl. Phys. 11, 607 (1970)]; C. F. Cho and J. J. Sakurai, Phys. Rev. D 2, 577 (1970); C. F. Cho, *ibid.* 4, 194 (1971); J. J. Sakurai, invited talk at the Japan-U. S. Joint Seminar on Elementary Particles, SLAC, 1971 (unpublished).

[15]B. H. Kellett, Nucl. Phys. B35, 517 (1971); B35, 541 (1971); B38, 573 (1972).

[16]W.-K. Tung, Phys. Rev. Letters 23, 1531 (1969).

[17]T. Akiba, M. Sakuraoka, and T. Ebata, Nucl. Phys. B31, 381 (1971).

[18]Notice that our definition of ν, Eq. (2.6), differs by a factor of m from that of Ref. 2. Thus the dimensionless scaling functions are $\nu W_2/m^2$ and W_1 in our work.

[19]M. D. Scadron and H. F. Jones, Phys. Rev. 173, 1734 (1968).

[20]H. F. Jones and M. D. Scadron (unpublished); Nucl. Phys. B10, 17 (1969); W. A. Bardeen and W. K. Tung, Phys. Rev. 173, 1423 (1968).

[21]A. C. Hearn, Nuovo Cimento 21, 333 (1961).

[22]J. S. Ball, Phys. Rev. 124, 2014 (1961).

[23]J. Ballam *et al.*, Phys. Rev. Letters 24, 960 (1970).

[24]G. Buschhorn *et al.*, Phys. Rev. Letters 37B, 211 (1971).

[25]H. Hontebeyrie, C. Meyers, J. Procureur, and Ph. Salin, Phys. Letters 36B, 98 (1971).

[26]F. E. Close and J. F. Gunion, Phys. Rev. D 4, 742 (1971); 4, 1576 (1971).

[27]G. Wolf, rapporteur's talk, in *Proceedings of the International Symposium on Electron and Photon Interactions at High Energies, 1971,* edited by N. B. Mistry (Cornell Univ. Press, Ithaca, N.Y., 1971).

[28]G. B. West, Phys. Rev. Letters 24, 1206 (1970).

[29]N. R. S. Tait and J. N. J. White, Nucl. Phys. B43, 27 (1972).

[30]V. D. Mur, Sov. Phys. JETP 17, 1458 (1963); 18, 727 (1964); H. D. I. Abarbanel, F. E. Low, I. J. Muzinich, S. Nussinov, and J. H. Schwarz, Phys. Rev. 160, 1329

(1967); A. H. Mueller and T. L. Trueman, Phys. Rev. D 2, 953 (1970); J. B.Bronzan, I. S. Gerstein, B. W. Lee, and F. E. Low, Phys. Rev. 157, 1448 (1967).
[31]M. J. Creutz, S. D. Drell, and E. A. Paschos, Phys. Rev. 178, 2300 (1969); M. Damashek and F. J. Gilman, Phys. Rev. D 1, 1319 (1970); C. A. Dominguez, C. Ferro Fontan, and R. Suaya, Phys. Letters 31B, 365 (1970).
[32]T. P. Cheng and W.-K. Tung, Phys. Rev. Letters 24, 851 (1970).
[33]D. O. Caldwell *et al.*, Phys. Rev. Letters 25, 609 (1970); W. P. Hesse *et al.*, *ibid.* 25, 613 (1970); H. Meyer *et al.*, Phys. Letters 33B, 189 (1970); J. Ballam *et al.*, Phys. Rev. Letters 23, 498 (1969).
[34]T. A. Armstrong *et al.*, Phys. Letters 34B, 535 (1971); Phys. Rev. D 5, 1640 (1972).
[35]E. D. Bloom *et al.*, SLAC Report No. SLAC-PUB-653, 1969 (unpublished).
[36]G. Buschhorn *et al.*, Phys. Letters 37B, 207 (1971); R. L. Anderson *et al.*, Phys. Rev. Letters 25, 1218 (1970); A. M. Boyarski *et al.*, *ibid.* 26, 1600 (1971).
[37]H. Harari, Phys. Rev. Letters 20, 1395 (1968); P. G. O. Freund, *ibid.* 20, 235 (1968).
[38]H. Cheng and T. T. Wu, Phys. Rev. 183, 1324 (1969); J. D. Bjorken, J. Kogut, and D. Soper, Phys. Rev. D 3, 1382 (1971); H. Harari and J. D. Bjorken, in *Proceedings of the International Symposium on Electron and Photon Interactions at High Energies, 1971,* edited by N. B. Mistry (Cornell Univ. Press, Ithaca, N. Y., 1972).
[39]E. D. Bloom *et al.*, Phys. Rev. Letters 28, 516 (1972); D. E. Andrews *et al.*, Cornell Report No. CLNS-169, 1971 (unpublished); C. Driver *et al.*, Nucl. Phys. B38, 1 (1972).
[40]We are indebted to Dr. G. Shaw for a useful discussion of this point.

PHYSICAL REVIEW D VOLUME 7, NUMBER 1 1 JANUARY 1973

Transverse-Momentum Distributions in High-Energy Collisions*

L. M. Saunders† and Davison E. Soper
Joseph Henry Laboratories, Princeton University, Princeton, New Jersey 08540
(Received 22 June 1972)

The distribution in transverse momentum of particles produced in very high-energy hadronic collisions is studied using a general class of Gaussian models. The models are exactly soluble and readily compared with experiment, given the lowest moments of single-particle and two-particle distributions. Perhaps most important, they provide a simple framework for prototypes of specific dynamical schemes, such as multiperipheral or statistical models, in which the general trends and signatures of these schemes are readily apparent.

I. INTRODUCTION

In a high-energy collision of two hadrons there are two immediately noticeable features in general. One is the presence of many secondary particles and the other is the extremely limited transverse momentum of all particles.[1] It is the latter feature we wish to discuss here within a class of phenomenological models.

Consider a collision in which exactly N hadrons are produced in the final state and all final-state momenta are measured. Because the transverse momenta are usually small we choose to describe the momentum P^μ of each particle by its transverse momentum $\vec{P}=(P_x, P_y)$ and by its rapidity

$$\theta=\tfrac{1}{2}\ln[(E+P_z)/(E-P_z)].$$

The momenta $P_1^\mu, P_2^\mu, \ldots, P_N^\mu$ are labeled according to the order of particles in rapidity: $\theta_1 \leq \theta_2 \cdots \leq \theta_N$. Thus $\vec{p}_N$ is the transverse momentum of the leading fragment of the incident particle, $\vec{p}_1$ is transverse momentum of the most backward fragment of the target particle, and so forth. The object to be discussed is the distribution of the transverse momenta,

$$\frac{1}{\sigma_N}\frac{d\sigma_N}{d\vec{p}_1\cdots d\vec{p}_N} = \frac{1}{\sigma_N}\int_{\theta_i<\theta_{i+1}} d\theta_1\cdots d\theta_N \frac{d\sigma_N}{d\theta_1 d\vec{p}_1\cdots d\theta_N d\vec{p}_N}. \tag{1}$$

Implicit in the assertion that the transverse-momentum distribution (1) is a useful object to study is the assumption that the transverse momenta are weakly correlated with the rapidities. We expect that it may be important to distinguish the particles by their order in rapidity, but that the precise values of the rapidities do not have much influence on the transverse-momentum distributions. This assumption is not wholly without foundation. Because of the transverse damping and because the average number of particles produced, $\langle N\rangle$, is small compared to E/m_π (typically $\langle N\rangle \sim \ln E$),[2] where E is the total center-of-mass energy, little correlation is introduced by over-all energy conservation. Furthermore, the absence of strong correlations is kinematically suggested in any sys-